
Beyond Token Eviction: Mixed-Dimension Budget Allocation for Efficient KV Cache Compression

Ruijie Miao^{*1} Zhiming Wang^{*1} Wang Li^{*1} Shiwei Wu² Shufan Liu² Yanbing Jiang¹ Tong Yang¹

Abstract

Key-value (KV) caching is widely used to accelerate transformer inference, but its memory cost grows linearly with input length, limiting long-context deployment. Existing token eviction methods reduce memory by discarding less important tokens, which can be viewed as a coarse form of dimensionality reduction that assigns each token either zero or full dimension. We propose MixedDimKV, a mixed-dimension KV cache compression method that allocates dimensions to tokens at a more granular level, and MixedDimKV-H, which further integrates head-level importance information. Experiments on long-context benchmarks show that MixedDimKV outperforms prior KV cache compression methods that do not rely on head-level importance profiling. When equipped with the same head-level importance information, MixedDimKV-H consistently outperforms HeadKV. Notably, our approach achieves comparable performance to full attention on LongBench with only 6.25% of the KV cache. Furthermore, in the Needle-in-a-Haystack test, our solution maintains 100% accuracy at a 50K context length while using as little as 0.26% of the cache.

1. Introduction

Support for long context is emerging as a core capability of large language models (LLMs) (Comanici et al., 2025; Yang et al., 2025; Zeng et al., 2025), enabling complex tasks like information retrieval from large-scale documents. However, this capacity is often constrained by the KV cache, which stores the key-value states of the previous tokens to avoid re-computation. As the sequence length grows, the KV cache size increases linearly, leading to a massive memory footprint and memory access overhead during the decoding stage, which ultimately results in poor inference efficiency.

¹Peking University ²ByteDance Seed. Correspondence to: Tong Yang <yangtong@pku.edu.cn>.

Research community has explored tremendous methods for KV cache compression (Xiao et al., 2024; Chen et al., 2024; Tang et al., 2024a; Tu et al., 2024). Token eviction (Zhang et al., 2023; Xiao et al., 2023; Li et al., 2024) is one of the representative methods due to its simplicity, feasibility, and effectiveness. The key idea is to maintain the “important” tokens in the cache and evict “unimportant” ones. Recently, some works (Chang et al., 2024; Saxena et al., 2024; Chang et al., 2025) have explored the possibility of KV cache compression via dimensionality reduction, which compress the keys and values to a fixed dimension. Our inspiration comes from such a perspective: in the token eviction scheme, the evicted tokens can be considered as compressed to 0 dimensions, and the maintained tokens can be considered as maintaining the full dimensions. Therefore, the token eviction scheme can be regarded as a special case for dimensionality reduction scheme, where each token is compressed to either 0 dimension or full dimension. Then a natural question arises: *Can we allocate dimensions to tokens at a more granular level to maximize information retention under a fixed budget?*

We propose MixedDimKV, a novel KV cache compression scheme that enables fine-grained budget allocation. As illustrated in Figure 1, our framework operates on a pre-defined set of candidate compression ratios, specifying the fractional budgets for keys and values. Then our solution efficiently prunes the KV cache by assigning more dimensions to keys and values that are most sensitive to information loss. To utilize every bit of budget space as efficiently as possible while considering inference computational efficiency, we have made the following designs:

Measuring information loss via attention output. To determine the optimal dimensionality for each token, we establish a scoring metric that quantifies the deviation induced by compression. Our methodology is centered on the joint impact of a token’s attention significance, value magnitude, and inherent compressibility across varying dimensions. While traditional methods often rely on attention weights to select tokens, which only consider the impact of keys, our approach evaluates the attention output directly to capture how these three factors interact to determine actual information loss. Based on this analysis, we design our met-

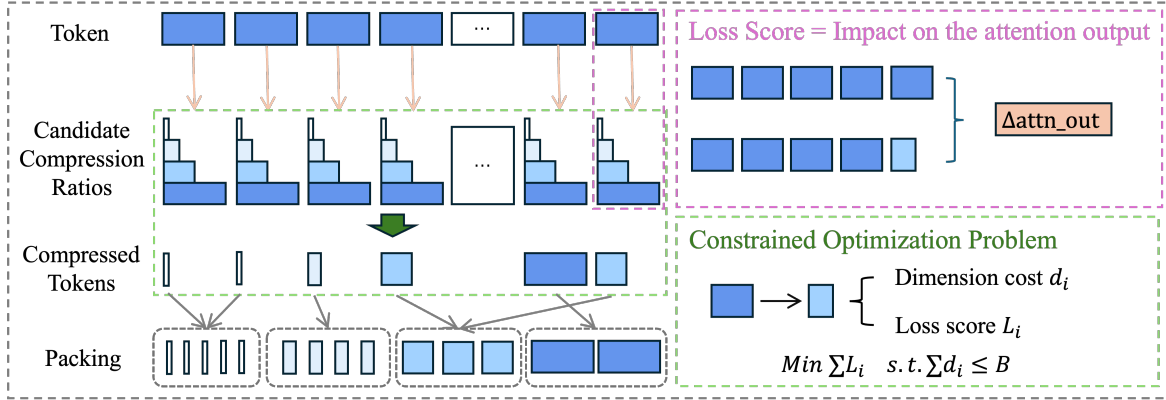


Figure 1. The two-stage dimension allocation process for KV cache compression. Candidate compression ratios are evaluated for each token to compute loss scores. An optimization objective is then applied to minimize total loss under the specified memory budget.

ric as a conservative estimation, specifically the upper bound of the deviation of the attention output, to ensure maximum information retention for critical tokens. This formulation is further optimized for efficient batched computation, ensuring that our fine-grained dimension allocation remains scalable even for extremely long sequences.

Optimal dimension allocation via bisection search. Leveraging the computed loss scores, we formulate the dimension allocation task as a constrained optimization problem, aiming to minimize the aggregate accuracy loss under a memory budget. While such discrete problems are generally challenging, we show that in long-context settings, the duality gap between the primal problem and its Lagrangian dual becomes negligible. By exploiting the monotonic relationship between allocated dimensionality and accuracy loss, we employ an efficient bisection-based search to determine the optimal per-token dimensions.

In implementing MixedDimKV, we favor head-wise compression over joint-head compression to strike a balance between allocation flexibility and computational efficiency. Furthermore, to ensure compatibility with established head-level importance estimation schemes, we propose a variant, MixedDimKV-H. On LongBench and RULER, MixedDimKV significantly outperforms prior methods without head-level profiling, while MixedDimKV-H consistently exceeds HeadKV when using the same head-level information. Notably, our approach achieves comparable performance to full attention on LongBench with only 6.25% (KV size = 512) of the KV cache. In the Needle-in-a-Haystack test, our solution maintains 100% accuracy at a 50K context length while using as little as 0.26% (KV size = 128) of the cache. Furthermore, our solution is highly efficient, reducing per-token decoding latency to 55% of full attention.

2. Related Works

Token eviction. A common KV cache compression strategy is to analyze token importance and evict the less important ones. StreamingLLM (Xiao et al., 2023) marks the initial tokens and the tokens in the recent window as important. H2O (Zhang et al., 2023) identifies important tokens via cumulative attention scores and dynamically updates KV cache. SnapKV (Li et al., 2024) scores the token importance based on the attention score with an observation window. PyramidKV (Cai et al., 2024) ranks tokens in the lower layer as more important and allocates more budget. HeadKV (Fu et al., 2024) further evaluates the importance of individual heads and incorporates these estimates into KV cache allocation process.

Dimension reduction. Several previous works have recognized the low-rank nature of KV cache and leveraged it for compression. Palu (Chang et al., 2024) proposes a low-rank decomposition for the linear projection matrices, which naturally reduces the hidden dimension of KV cache. Eigen Attention (Saxena et al., 2024) conducts low-rank decomposition on KV cache and proposes a layer-wise rank allocation algorithm to decide each layer’s compression ratio. ShadowKV (Sun et al., 2024) conducts low-rank decomposition for pre-RoPE keys, which requires reconstructing them during the decoding stage. None of these works has considered assigning different ranks to tokens with varying levels of importance.

Sparse attention. Some works store the entire KV cache but dynamically load a small portion of KV during the decoding stage. Quest (Tang et al., 2024b) approximates keys by the channel-wise minimal and maximal values and selects important pages of tokens by estimating attention weights. SparQ (Ribar et al., 2023) selects important channels of keys to estimate attention weights, and then fetches keys and values with high contribution. PQCache (Zhang et al., 2025) applies Product Quantization techniques to retrieve

top-k relevant key-value pairs.

Quantization. Many works compress KV cache by reducing the bit width. KVQuant (Hooper et al., 2024) applies several techniques to achieve a 3-bit quantization. PolarQuant (Wu et al., 2025) encodes KV caches with quantized radii and angles. While these works achieve good performance, they are orthogonal to our method.

3. Preliminary

3.1. Attention Mechanism and KV Cache

In transformer-based models, the multi-head attention (MHA) module with H heads projects the input sequence of embeddings into H sets of queries, keys, and values. The attention output for each head i is computed as:

$$\text{Attn}(Q_i, K_i, V_i) = \text{softmax}\left(\frac{Q_i K_i^\top}{\sqrt{d}}\right) V_i$$

During the decoding stage, to avoid excessive recomputation for the keys and values of previous tokens, the key-value pairs are cached. The memory overhead of KV cache scales linearly with the number of heads and sequence length, leading to prohibitive memory costs.

To mitigate this, grouped-query attention (GQA) (Ainslie et al., 2023) partitions the H query heads into G groups. Within each group, multiple queries share one key and value head. By reducing the number of KV heads from H to G , the KV cache size is substantially reduced. Many recent LLMs (Yang et al., 2025; Jiang et al., 2023; Grattafiori et al., 2024) have applied GQA architecture in their models.

3.2. Principal Component Analysis

We employ Principal Component Analysis (PCA) (Abdi & Williams, 2010) algorithm to compress the KV cache. Specifically, for a key matrix $K \in \mathbb{R}^{n \times d}$, PCA performs singular value decomposition on the covariance-like matrix $K^\top K/n$, yielding $K^\top K/n = U \Sigma U^\top$. To achieve a ρ compression ratio, we construct a projection matrix $P_K = U_r \in \mathbb{R}^{d \times r}$, where U_r consists of the first $r = d \cdot \rho$ columns of U corresponding to the largest eigenvalues. The original key K is projected to a lower-dimensional representation $K_c = K \cdot P_K \in \mathbb{R}^{n \times r}$. Similarly, the value matrix V is compressed into $V_c = V P_V$ using its respective projection matrix P_V . Our method reduces the KV cache storage from $2nd$ to $2nr$, and also introduces a fixed overhead of $2dr$ to store the projection matrices.

During inference, we first project the query q into the r -dimensional subspace: $\hat{q} = q P_K$. The attention weights are then efficiently computed in this reduced space. After obtaining the weighted sum of compressed values V_c , we project the result back to the original d -dimensional space.

Table 1. Comparison of head-wise and joint-head compression. Head-wise compression reduces projection overhead and enhances inference efficiency. Its support for head-level budget allocation ensures competitive compression performance.

Granularity	Projection Matrices Overhead	Computational Efficiency	Compression Quality
Joint-head	×	×	✓
Head-wise	✓	✓	✓

The complete process is formulated as

$$\text{Attn}(q, K_c, V_c) = \text{softmax}\left(\frac{q P_K K_c^\top}{\sqrt{d}}\right) V_c P_V^\top$$

4. Solution

To process the KV cache of a user prompt, we partition the prompt into a local window Q consisting of the last α tokens and the remaining tokens. The local window is fully retained (i.e., 100% compression ratio), while the remaining tokens are assigned compression ratios from a predefined candidate set. To maximize performance under a KV cache budget, we prioritize higher dimensions for important, less compressible tokens. For dimension reduction, we apply PCA to each head independently rather than across all heads jointly, owing to the superior efficiency and flexibility (Section 4.1). We quantify the impact of compression by computing an accuracy loss score, defined as the deviation in attention output, for each token-dimension pair (Section 4.2). The dimension allocation is then formulated as a constrained optimization problem, which we solve using an efficient search algorithm to find the optimal assignment (Section 4.3).

4.1. Head-wise Compression

Let H_{kv} be the number of KV heads, N be the number of tokens in the KV cache, and D be the head dimension. We denote $X \in \mathbb{R}^{H_{kv} \times N \times D}$ as either the key or value cache. There are two ways to conduct PCA for X .

- Head-wise compression.** We make dimensional reduction for each head individually. On each head, we compress dimensions from D to a specific ratio.
- Joint-head compression.** Heads are concatenated to form $X_{joint} \in \mathbb{R}^{N \times (H_{kv} \cdot D)}$. We compress dimensions from $H_{kv} \cdot D$ to a specific ratio.

Although prior work (Chang et al., 2024) has observed a better low-rank property for joint-head compression, it may not lead to overall performance improvement. As summarized in Table 1, head-wise compression consistently exceeds or matches joint-head compression across multiple aspects. We justify this choice through the following three factors.

First, head-wise compression is more memory-efficient regarding projection matrices. For a compression ratio ρ , head-wise compression brings an overhead of $H_{kv}D^2\rho$, while joint-head compression requires $(H_{kv}D)^2\rho$, which is $H_{kv}\times$ higher. For a GQA model ($H = 32$, $H_{kv} = 8$, $D = 128$) at a compression ratio of $\rho = 25\%$, the joint-head overhead is equivalent to storing 64 full tokens per layer per head, which is prohibitive for constrained budget settings (e.g., 128 tokens).

Second, joint-head compression brings higher computation complexity. Since attention is a head-level operation, joint-head compression requires either reconstructing the full KV cache, which negates any efficiency gains, or operating on a joint subspace. For example, at $\rho = 25\%$ with 8 heads, the joint dimension becomes $2\times$ the original head dimension, increasing rather than decreasing the per-head computational burden.

Third, and most importantly, joint-head compression enforces uniform behavior across all heads, ignoring the non-uniform importance across heads. Recent work (Fu et al., 2024) has pointed out that allocating non-uniform budgets to different heads can yield better performance. Head-wise compression naturally supports this spatial adaptivity, whereas the gains from joint-head low-rankness are often canceled out by the lack of head-level adaptivity, which is confirmed by experiments in Section 6.5.

4.2. Accuracy Loss Score

To assess the impact of compressing a specific token, we employ an analysis that isolates the error introduced by the t^{th} token, assuming all other tokens remain unchanged. We target at the change of attention output for queries in the local window Q and formulate it as $\sum_{q \in Q} \|p'_{q,t}V'_t - p_qV\|_2$, where $p_{q,t}$ refers to the attention scores for query q with the changed t^{th} token, and V'_t refers to the values with changed t^{th} entry. Given that the local window provides only a partial sampling of the queries, we adopt a conservative score estimation to ensure that critical tokens retain their original information as much as possible. We consider the upper bound

$$\sum_{q \in Q} \|\Delta p_{q,t}V\|_2 + \|p'_{q,t}\Delta V\|_2$$

To simplify the computation and facilitate efficient batched processing, we consider all tokens to be compressed at a specific ratio, yielding attention score p'_q for query q . Due to the low-rankness of the key-values and the sparsity of attention scores, we regard the p'_q to be a slight perturbation of $p_{q,t}$. Therefore, we define the scoring metric as

$$L_t = \sum_{q \in Q} \|(p'_q - p_q)^{(t)} \cdot V^{(t)}\|_2 + \|p_q^{(t)} \cdot (V' - V)^{(t)}\|_2$$

Algorithm 1 Loss Score Computation

Input: Key $K \in \mathbb{R}^{N \times d}$, Value $V \in \mathbb{R}^{N \times d}$, Query $Q \in \mathbb{R}^{M \times d}$, compression ratio ρ , head dimension d
Output: Loss score vector $\mathbf{L} \in \mathbb{R}^N$

$P \leftarrow \text{Softmax}(\frac{QK^T}{\sqrt{d}})$ // $P \in \mathbb{R}^{M \times N}$

if $\rho == 0\%$ **then**
 $E \leftarrow 2 \cdot P \odot \|V\|_2$

else if $\rho == 100\%$ **then**
 $E \leftarrow \mathbf{0}_{M \times N}$

else
 $K', V' \leftarrow \text{Compressed}(K, V, \rho)$
 $P' \leftarrow \text{Softmax}(\frac{QK'^T}{\sqrt{d}})$
 $E \leftarrow |P' - P| \odot \|V\|_2 + P \odot \|V - V'\|_2$

end if
 $\mathbf{L} \leftarrow \sum_{i=1}^M E[i, :]$ // Sum across queries

Then we can efficiently compute the scores for the entire input sequences in batches. As shown in Algorithm 1, we first compute the error matrix $E = |P' - P| \cdot \|V\|_2 + P \cdot \|V - V'\|_2$, where E_{ij} estimates the impact of the j -th token on the i -th query's output. Then we compute the loss score by summing across queries, i.e., $L = \sum_{i=1}^M E[i, :]$. Our algorithm also accounts for two boundary cases where the compression ratio ρ is either 100% or 0%. When $\rho = 100\%$, i.e., no compression is applied, we simply set the error matrix to zero. When $\rho = 0\%$, i.e., evicted tokens, we zero out both the attention weights and the value vectors, yielding an error matrix of $2 \cdot P \odot \|V\|_2$.

Generalization of Token Eviction. SnapKV (Li et al., 2024) focuses on token eviction by retaining only those tokens with the highest attention weights within an observation window. If we set the candidate compression ratios to $\{0\%, 100\%\}$, our solution also functions as token eviction. In such a case, to minimize the total loss score, tokens with highest $\sum_{q \in Q} p_q^{(t)} \|V^{(t)}\|_2$ are maintained. Compared to SnapKV, our accuracy loss score incorporates both attention importance and value magnitudes, offering a more nuanced sensitivity metric for cache management.

4.3. Latent dimension allocation

With token-wise loss scores computed, we then select the optimal dimension for each token to minimize the total loss while adhering to the KV cache budget. Let \mathcal{D} denote the set of candidate dimensions, $d_i \in \mathcal{D}$ be the dimension allocated to the i -th token, $L_i(d_i)$ be the corresponding accuracy loss, and B be the total budget. The allocation is formulated as a constrained discrete optimization problem:

$$\min_{\{d_i \in \mathcal{D}\}_{i=1}^N} \sum_{i=1}^N L_i(d_i) \quad \text{s.t.} \quad \sum_{i=1}^N d_i \leq B. \quad (1)$$

Although the problem is non-convex due to the discrete domain, the primal–dual gap is negligible, especially for long-context scenarios.

Theorem 4.1. *The gap between Equation (1) and its Lagrangian dual is bounded by a small constant Δ independent of the sequence length N .*

We defer the proof and related discussion in Section A. Therefore, we consider its Lagrangian dual:

$$\max_{\lambda \geq 0} \min_{\{d_i\}} \left(\sum_{i=1}^N L_i(d_i) + \lambda \left(\sum_{i=1}^N d_i - B \right) \right) \quad (2)$$

For a fixed λ , the optimization decouples into N independent sub-problems:

$$d_i^*(\lambda) = \arg \min_{d \in \mathcal{D}} (L_i(d) + \lambda d) \quad (3)$$

We adopt the natural assumption that $L_i(d)$ is monotonically decreasing with respect to d , as higher-dimensional representations typically preserve more information. Consequently, a higher λ encourages selecting a smaller d , making the total budget consumption $C(\lambda) = \sum_i d_i^*(\lambda)$ a monotonically non-increasing step function of λ . This monotonicity allows us to efficiently find the optimal λ^* via bisection search. In each iteration, we update λ and determine the corresponding $\{d_i^*\}$ until the aggregate budget $C(\lambda)$ converges to the target B .

4.4. Inter-head vs. Intra-head Optimization

Our proposed framework is highly versatile and can operate under two distinct settings depending on the availability of external information.

If no external information on the importance of layers and heads is given, the basic MixedDimKV distributes the budget evenly across all layers. The optimization problem in Equation (1) is formulated across all heads and tokens within a single layer. By solving this problem, the basic MixedDimKV inherently enables joint budget allocation at both the inter-head and inter-token levels. If some heads have a higher impact on the attention output, they will be allocated a higher budget.

MixedDimKV is also compatible with existing methods that provide explicit importance of layers and heads. HeadKV (Fu et al., 2024) profiles head-level importance by contextual QA tasks, and partitions the total budget among heads of all layers according to their estimated saliency. We can retain the head-level quotas established by HeadKV, while employing our mixed-dimension optimization scheme to refine the token-wise distribution within each head. Under this setting, the optimization problem in Equation (2) is formulated independently for each head, focusing on intra-head token selection. We denote this variant as MixedDimKV-H.

5. Implementation

In this section, we discuss the practical implementation of our solution, focusing on memory layout and projection matrix management.

To optimize the memory layout and the computational efficiency, we reorganize the compressed KV cache by packing tokens with identical dimensions into contiguous tensors. This layout enables vectorized attention kernels to operate on each group independently, with the results aggregated subsequently. To avoid excessive memory fragmentation and kernel launch overhead, we limit the number of candidate ratios. Although this rearranges the physical memory, mathematical correctness is preserved as the positional information (e.g., RoPE) is already explicitly embedded within the representations.

Regarding projection storage, we exploit the nested structure of our matrices. Since projection bases are derived from the eigenvectors of $K^\top K/N$ and $V^\top V/N$ through truncation, the basis for a lower dimension is a subset of the higher-dimension one. Consequently, we only store the maximum-rank projection matrix (for the largest $\rho < 100\%$). Any lower-rank matrix is obtained by simply slicing the maximum matrix, reducing the fixed memory footprint.

6. Experiments

6.1. Setup

Models and Datasets. We conduct experiments on open-sourced state-of-the-art LLMs: Llama-3-8B-Instruct (Grattafiori et al., 2024), the long-context finetuned variant Llama-3-8B-Instruct-Gradient-1048K (Gradient AI, 2024), and Mistral-7B-Instruct-v0.3 (Jiang et al., 2023). We compare our solution with baselines on representative benchmarks, including Longbench (Bai et al., 2024), RULER (Hsieh et al., 2024), and Needle-in-a-Haystack (Kamradt, 2023). The experiments are conducted on NVIDIA A100 80GB GPUs.

Baselines. We use the following baselines:

- H2O (Zhang et al., 2023) applies an update policy to maintain a set of heavy-hitter tokens.
- SnapKV (Li et al., 2024) uses an observation window consisting of the last α tokens to compute attention scores of the remaining tokens. Tokens with a higher sum of attention scores are maintained in the KV cache.
- PyramidKV (Cai et al., 2024) allocates more budget to lower layers and less budget to higher layers, and within each layer it applies SnapKV for KV selection.
- HeadKV (Fu et al., 2024) allocates budget to each head according to the head’s importance, and for each head, it applies SnapKV for KV selection.

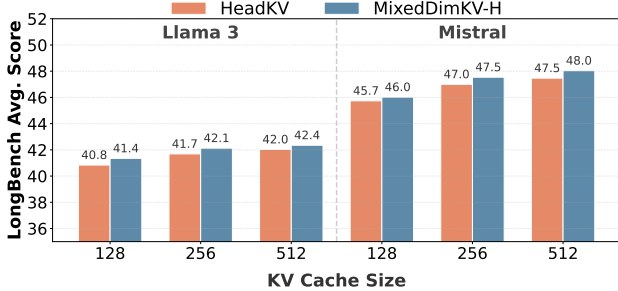


Figure 2. Comparison of HeadKV and MixedDimKV-H.

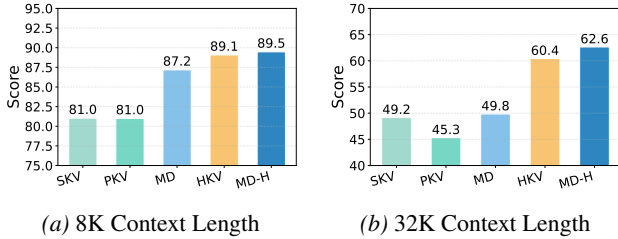


Figure 3. Performance comparison on RULER. The terms ‘SKV’, ‘PKV’, ‘MD’, ‘HKV’, ‘MD-H’ denote SnapKV, PyramidKV, MixedDimKV, HeadKV, MixedDimKV-H, respectively.

Both our solution and many of the baselines will sample α last tokens for further KV cache compression, and for fairness we set α the same for all solutions in one experiment. PyramidKV involves a parameter β to control the layer-wise budget allocation, and we set $\beta = 20$ as recommended in its paper. HeadKV involves a parameter β to control the head-wise budget allocation, and we set $\beta = 1.1$ for both HeadKV and MixedDimKV-H, which is one of the recommended parameter settings in its paper. When computing the KV budget consumption, the projection matrices are also counted in our solution. We set the candidate compression ratios to $\{0\%, 12.5\%, 25\%, 100\%\}$, and we discuss this choice in Section B.

Beyond the general comparisons above, we further evaluate MixedDimKV against Palu, the SOTA solution that focuses on KV cache dimension reduction. The detailed results are presented in Section C.3.

6.2. Main Results on Long-Context Benchmarks

We evaluate our solution on long-context benchmarks, including LongBench and RULER.

We evaluate performance on LongBench using equivalent KV sizes of 128, 256, and 512. Following (Cai et al., 2024; Fu et al., 2024), a KV size T denotes a total budget of $H \times T \times D$, where H is the number of heads and D is the head dimension. Since our approach introduces dimension reduction and projection overhead, this metric represents the equivalent memory budget rather than raw token counts.

Due to space constraints, we present primary results here and provide the full results in Section C.1.

As shown in Table 2, MixedDimKV significantly outperforms baselines lacking head-level importance profiling (H2O, SnapKV, PyramidKV), especially under tight budgets (KV size = 128). At a KV size of 512, MixedDimKV matches full-attention performance on Llama-3. Figure 2 further shows that MixedDimKV-H consistently exceeds HeadKV using identical head-importance profiling data, confirming the efficacy of mixed-dimension compression. Notably, even without profiling, MixedDimKV outperforms HeadKV at 128 KV size on both Llama-3 (41.07 vs. 40.84) and Mistral (46.56 vs. 45.74). We attribute this to HeadKV’s reliance on static, offline metrics derived from extensive Needle-in-a-Haystack tests. While these metrics capture general head importance, they fail to identify which heads are more critical within the current KV cache context. In contrast, our method dynamically adapts to the current input, enabling more precise head-level allocation when resources are limited.

Figure 3 presents the comparison of the average score on RULER with context lengths of 8K and 32K, using a fixed KV cache size of 256. We omit H2O from the visualization due to its significantly lower scores, and the full results can be found in Section C.2. The results on RULER exhibit a similar trend. MixedDimKV consistently surpasses SnapKV and PyramidKV in overall performance. Notably, in the more challenging 32K setting, MixedDimKV-H not only achieves the highest score but also broadens its lead over the competitive HeadKV baseline, reaching a peak performance of 62.64. This indicates our mixed-dimension compression enables more efficient memory usage when the budget is extremely limited.

6.3. Needle-in-a-Haystack Test

We evaluate the long-context information retrieval performance of different KV cache compression schemes using the Needle-in-a-Haystack test. For Llama-3-8B-Instruct-1048k, we set the maximum context length to 50K, the KV size to 128, and the query window size to 32. As shown in Figure 4, our solution successfully retrieves important information under long-context scenarios. MixedDimKV significantly outperforms the baselines that do not rely on additional head-level information (SnapKV, PyramidKV), and achieves a score close to HeadKV, which requires a time-consuming profiling process. Equipped with the same head-level information, MixedDimKV-H achieves a 100 score and outperforms HeadKV, indicating our mixed-dimension compression scheme is beneficial to the space utility of KV cache. In Section C.4 we present the Needle-in-a-Haystack results on Mistral-7B-Instruct, which show the same trend as on Llama-3-8B-Instruct-1048K.

Beyond Token Eviction: Mixed-Dimension Budget Allocation for Efficient KV Cache Compression

Table 2. Performance comparison on LongBench. MixedDimKV (MD) is compared against KV cache compression methods that do not rely on additional head-level importance profiling.

Method	Single-Doc QA			Multi-Doc QA			Summarization			Few-shot Learning			Synthetic		Code		Avg.
	NQA	Qasper	MF-en	HQA	2WQA	Musq	GRep	QMSum	MNews	TREC	TQA	SAMSum	PCount	PRe	Lcc	RB-P	
<i>Llama-3-8B-Instruct KV size = 128</i>																	
Full	25.56	32.30	39.71	43.56	35.49	21.14	28.58	23.22	26.67	74.00	90.48	42.29	4.80	69.75	59.13	54.02	41.92
H2O	23.52	13.74	25.26	29.07	22.72	14.67	21.94	21.34	24.01	46.50	87.99	35.12	5.36	68.21	54.77	48.73	33.93
SnapKV	22.39	15.98	30.97	40.78	28.60	19.35	19.76	21.88	21.40	65.50	89.72	38.77	5.75	69.00	58.76	54.73	37.71
Pyramid	21.40	16.92	31.62	38.45	28.72	18.59	19.97	22.48	20.96	66.50	89.35	38.39	5.92	69.00	57.86	51.80	37.37
MD	25.22	29.07	38.30	43.20	33.84	19.58	24.53	23.12	26.03	72.00	90.61	42.16	5.54	69.50	59.32	55.16	41.07
<i>Llama-3-8B-Instruct KV size = 512</i>																	
Full	25.56	32.30	39.71	43.56	35.49	21.14	28.58	23.22	26.67	74.00	90.48	42.29	4.80	69.75	59.13	54.02	41.92
H2O	23.76	21.56	31.57	40.54	30.36	17.79	24.89	22.15	25.74	69.00	90.67	40.33	6.05	68.07	61.00	56.26	39.36
SnapKV	25.53	23.59	38.58	43.78	33.33	19.85	23.10	22.52	24.19	71.00	90.57	40.48	5.51	69.50	61.10	57.23	40.62
Pyramid	24.83	23.33	35.20	43.29	31.87	20.55	23.43	22.80	24.29	71.50	90.61	40.81	5.91	69.50	59.60	54.71	40.14
MD	25.56	32.11	39.71	43.56	35.55	21.18	28.66	23.29	26.70	73.50	90.48	42.47	4.80	69.25	59.15	54.13	41.88
<i>Mistral-7B-Instruct KV size = 128</i>																	
Full	29.07	41.54	52.88	49.37	39.01	28.58	35.07	25.71	27.73	76.00	88.59	47.51	6.00	98.50	61.48	62.68	48.11
H2O	26.48	29.11	37.10	45.26	32.37	22.33	25.20	20.91	25.02	68.50	86.04	38.79	5.50	81.50	47.28	45.06	39.78
SnapKV	26.78	30.63	48.03	47.58	35.09	25.35	21.90	22.12	21.83	69.50	88.59	43.91	6.00	94.00	55.70	55.14	43.26
Pyramid	26.65	29.71	48.84	48.01	35.85	25.06	22.31	22.36	21.17	68.00	88.80	43.87	4.50	94.00	55.39	52.57	42.94
MD	29.88	38.09	51.57	48.91	38.40	26.95	27.12	25.08	27.03	69.50	88.81	47.44	5.50	98.00	61.25	61.45	46.56
<i>Mistral-7B-Instruct KV size = 512</i>																	
Full	29.07	41.54	52.88	49.37	39.01	28.58	35.07	25.71	27.73	76.00	88.59	47.51	6.00	98.50	61.48	62.68	48.11
H2O	26.95	35.27	43.65	47.13	35.25	23.68	28.70	22.72	26.51	74.50	88.76	42.92	5.50	91.00	57.08	52.08	43.86
SnapKV	29.22	36.49	54.05	49.70	38.72	26.72	26.01	24.24	25.26	75.00	89.44	46.85	5.00	96.00	60.27	60.66	46.48
Pyramid	27.86	36.07	52.99	49.35	38.10	26.97	25.67	23.91	24.92	73.50	89.91	45.83	5.00	96.50	59.37	59.20	45.95
MD	30.06	38.72	52.04	48.30	38.64	27.20	27.86	25.26	27.20	72.00	88.81	47.39	5.50	97.50	61.52	61.64	46.85

6.4. Inference Efficiency

In this section, we implement our solution in FlashAttention (Dao, 2023) and evaluate the inference efficiency on Llama-3-8B-Instruct-1048K. Figure 5 reports decoding latency for 128K inputs across varying generation lengths, and peak memory usage across different context lengths with generation length set to 1. We construct these inputs from the Needle-in-a-Haystack dataset. When the generation length is 1, the decoding latency represents the pre-filling latency, and our solution introduces minimal overhead, with latency only slightly higher than full attention (around 5s for 128K input). For a generation length of 4096, our solution reduces total and per-token latency to 61.31% and 55.18% of the baselines, respectively. With 128K contexts, our solution lowers the peak memory usage to 66.44%.

6.5. Ablation Study

In this section, we further conduct extensive ablation studies. By comparing head-wise and joint-head compression schemes, we show that joint-head compression does not outperform head-wise compression. We also evaluate our

solution under different numbers of candidate dimensions, indicating that a more fine-grained compression leads to better performance. In Section C.5 we report the number of tokens compressed to each dimension to guarantee it does not degenerate to the token eviction scheme. The following experiments are conducted on the LongBench with Llama-3-8B-Instruct.

Head-wise vs. joint-head compression. We conducted an ablation study by replacing head-wise compression with joint-head compression on keys to evaluate its impact. Because heads are combined for compression, the latent dimension allocation process only searches for an optimal token-level budget distribution. Both strategies share the same set of candidate dimension compression ratios and use no extra information of head-level importance. As shown in Figure 6, head-wise compression achieves much better performance under a low budget (e.g., 128 KV size), due to its reduced projection matrices overhead. Even with a higher budget size, the joint-head compression does not show an advantage. We believe this is because head-wise compression can distribute budget more flexibly as compression is conducted at the head-level.

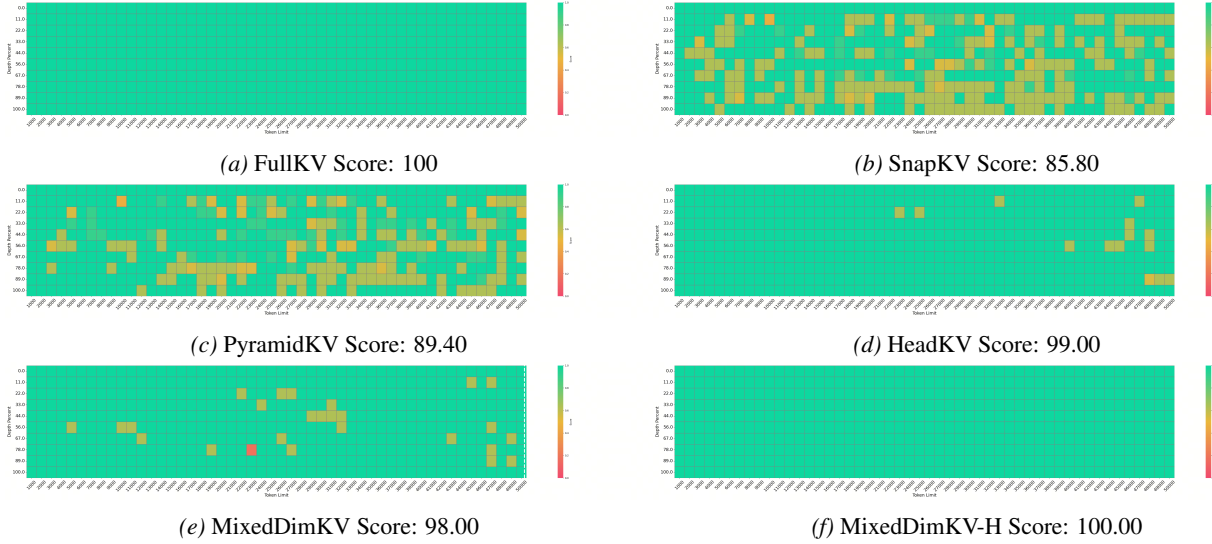


Figure 4. Results of Needle-in-a-Haystack test on Llama-3-8B-Instruct-1048K with KV size 128.

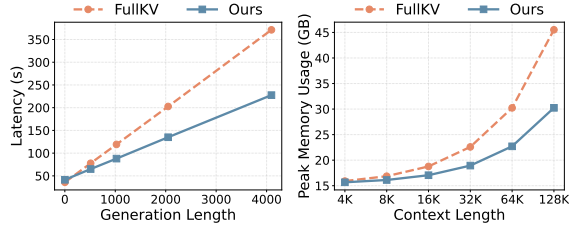


Figure 5. Decoding latency and peak memory usage.

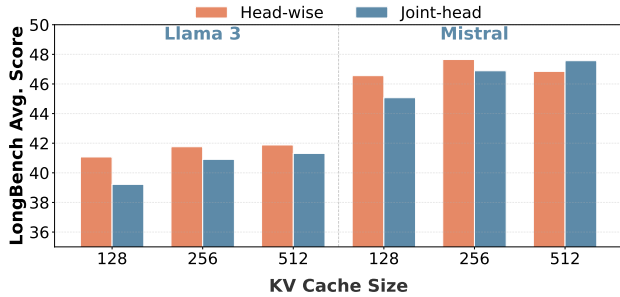


Figure 6. Comparison of head-wise and joint-head compression.

Granularity of mixed-dimension ratios. We investigate the influence of dimension granularity by evaluating two candidate ratio sets: $\{0\%, 100\%\}$ and $\{0\%, 12.5\%, 25\%, 100\%\}$, which represent mixed-dimension compression at varying levels of granularity. We set the KV size to 256, and use SnapKV as the baseline. As shown in Table 3, $\{0\%, 100\%\}$ outperforms the SnapKV baseline, and we attribute the superior performance to two advantages. First, our solution adopts a more rational score design that incorporates value information, while SnapKV only considers the impact of keys. Second, our dimension

Table 3. Comparison of SnapKV and MixedDimKV with two granularity of candidate ratio sets: $\{0\%, 100\%\}$, and $\{0\%, 12.5\%, 25\%, 100\%\}$.

Method	SnapKV	$\{0\%, 100\%\}$	$\{0\%, 12.5\%, 25\%, 100\%\}$
Score	39.77	40.93	41.76

allocation mechanism inherently supports distinct budget ratios for different attention heads, in contrast to SnapKV, which enforces identical budget consumption across all heads. Moreover, the performance leap from $\{0\%, 100\%\}$ to $\{0\%, 12.5\%, 25\%, 100\%\}$ indicates that progressively finer-grained dimension ratio design leads to better results.

7. Conclusion

In this paper, we present MixedDimKV, an efficient KV cache compression scheme. MixedDimKV maximizes the budget utilization by compressing tokens to suitable dimensions based on their impact on the attention output. When information of head-level importance is available, we further propose MixedDimKV-H, which combines the benefits of mixed-dimension compression and head-level budget allocation. Experiments on long-context benchmarks show that MixedDimKV significantly outperforms prior methods without head-level profiling, while MixedDimKV-H consistently exceeds HeadKV. On an A100, MixedDimKV reduces the per-token decoding latency to 55% compared with full attention. These results demonstrate that MixedDimKV significantly alleviates the memory bottleneck of LLMs, thereby extending the scalability of LLMs to long-context tasks within limited hardware budgets.

Impact Statement

This paper presents work whose goal is to advance the field of Machine Learning, and more specifically, the resource-efficiency of LLM inference. Our solution facilitates the efficient deployment of LLMs in resource-constrained environments, thereby democratizing access to cutting-edge AI for small organizations and independent researchers. As a technical optimization for KV cache efficiency, this work does not introduce new ethical concerns or negative societal consequences regarding its deployment or use.

References

- Abdi, H. and Williams, L. J. Principal component analysis. *Wiley interdisciplinary reviews: computational statistics*, 2(4):433–459, 2010.
- Ainslie, J., Lee-Thorp, J., De Jong, M., Zemlyanskiy, Y., Lebrón, F., and Sanghai, S. Gqa: Training generalized multi-query transformer models from multi-head checkpoints. *arXiv preprint arXiv:2305.13245*, 2023.
- Bai, Y., Lv, X., Zhang, J., Lyu, H., Tang, J., Huang, Z., Du, Z., Liu, X., Zeng, A., Hou, L., et al. Longbench: A bilingual, multitask benchmark for long context understanding. In *Proceedings of the 62nd Annual Meeting of the Association for Computational Linguistics (Volume 1: Long Papers)*, pp. 3119–3137, 2024.
- Cai, Z., Zhang, Y., Gao, B., Liu, Y., Li, Y., Liu, T., Lu, K., Xiong, W., Dong, Y., Hu, J., et al. Pyramidkv: Dynamic kv cache compression based on pyramidal information funneling. *arXiv preprint arXiv:2406.02069*, 2024.
- Chang, C.-C., Lin, W.-C., Lin, C.-Y., Chen, C.-Y., Hu, Y.-F., Wang, P.-S., Huang, N.-C., Ceze, L., Abdelfattah, M. S., and Wu, K.-C. Palu: Compressing kv-cache with low-rank projection. *arXiv preprint arXiv:2407.21118*, 2024.
- Chang, C.-C., Lin, C.-Y., Akhauri, Y., Lin, W.-C., Wu, K.-C., Ceze, L., and Abdelfattah, M. S. xkv: Cross-layer svd for kv-cache compression. *arXiv preprint arXiv:2503.18893*, 2025.
- Chen, Z., Sadhukhan, R., Ye, Z., Zhou, Y., Zhang, J., Nolte, N., Tian, Y., Douze, M., Bottou, L., Jia, Z., et al. Magicpig: Lsh sampling for efficient llm generation. *arXiv preprint arXiv:2410.16179*, 2024.
- Comanici, G., Bieber, E., Schaekermann, M., Pasupat, I., Sachdeva, N., Dhillon, I., Blistein, M., Ram, O., Zhang, D., Rosen, E., et al. Gemini 2.5: Pushing the frontier with advanced reasoning, multimodality, long context, and next generation agentic capabilities. *arXiv preprint arXiv:2507.06261*, 2025.
- Dao, T. Flashattention-2: Faster attention with better parallelism and work partitioning. *arXiv preprint arXiv:2307.08691*, 2023.
- Fu, Y., Cai, Z., Asi, A., Xiong, W., Dong, Y., and Xiao, W. Not all heads matter: A head-level kv cache compression method with integrated retrieval and reasoning. *arXiv preprint arXiv:2410.19258*, 2024.
- Gradient AI. Llama-3-8b-instruct-gradient-1048k (revision 84c083a), 2024. URL <https://huggingface.co/gradientai/Llama-3-8B-Instruct-Gradient-1048k>.
- Grattafiori, A., Dubey, A., Jauhri, A., Pandey, A., Kadian, A., Al-Dahle, A., Letman, A., Mathur, A., Schelten, A., Vaughan, A., et al. The llama 3 herd of models. *arXiv preprint arXiv:2407.21783*, 2024.
- Hooper, C., Kim, S., Mohammadzadeh, H., Mahoney, M. W., Shao, Y. S., Keutzer, K., and Gholami, A. Kvquant: Towards 10 million context length llm inference with kv cache quantization. *Advances in Neural Information Processing Systems*, 37:1270–1303, 2024.
- Hsieh, C.-P., Sun, S., Kriman, S., Acharya, S., Rekish, D., Jia, F., Zhang, Y., and Ginsburg, B. Ruler: What’s the real context size of your long-context language models? *arXiv preprint arXiv:2404.06654*, 2024.
- Jiang, A. Q., Sablayrolles, A., Mensch, A., Bamford, C., Chaplot, D. S., de las Casas, D., Bressand, F., Lengyel, G., Lample, G., Saulnier, L., Lavaud, L. R., Lachaux, M.-A., Stock, P., Scao, T. L., Lavril, T., Wang, T., Lacroix, T., and Sayed, W. E. Mistral 7b, 2023. URL <https://arxiv.org/abs/2310.06825>.
- Kamradt, G. Needle in a haystack - pressure testing llms, 2023. URL https://github.com/gkamradt/LLMTest_NeedleInAHaystack.
- Li, Y., Huang, Y., Yang, B., Venkitesh, B., Locatelli, A., Ye, H., Cai, T., Lewis, P., and Chen, D. Snapkv: Llm knows what you are looking for before generation. *Advances in Neural Information Processing Systems*, 37:22947–22970, 2024.
- Ribar, L., Chelombiev, I., Hudlass-Galley, L., Blake, C., Luschi, C., and Orr, D. Sparq attention: Bandwidth-efficient llm inference. *arXiv preprint arXiv:2312.04985*, 2023.
- Saxena, U., Saha, G., Choudhary, S., and Roy, K. Eigen attention: Attention in low-rank space for kv cache compression. *arXiv preprint arXiv:2408.05646*, 2024.
- Starr, R. M. Quasi-equilibria in markets with non-convex preferences. *Econometrica*, 37(1):25–38, 1969. doi: 10.

2307/1909201. URL <https://www.jstor.org/stable/1909201>.

Sun, H., Chang, L.-W., Bao, W., Zheng, S., Zheng, N., Liu, X., Dong, H., Chi, Y., and Chen, B. Shadowkv: Kv cache in shadows for high-throughput long-context llm inference. *arXiv preprint arXiv:2410.21465*, 2024.

Tang, H., Lin, Y., Lin, J., Han, Q., Hong, S., Yao, Y., and Wang, G. Razorattention: Efficient kv cache compression through retrieval heads. *arXiv preprint arXiv:2407.15891*, 2024a.

Tang, J., Zhao, Y., Zhu, K., Xiao, G., Kasikci, B., and Han, S. Quest: Query-aware sparsity for efficient long-context llm inference. *arXiv preprint arXiv:2406.10774*, 2024b.

Tu, D., Vashchilenko, D., Lu, Y., and Xu, P. Vl-cache: Sparsity and modality-aware kv cache compression for vision-language model inference acceleration. *arXiv preprint arXiv:2410.23317*, 2024.

Wu, S., Lv, A., Feng, X., Zhang, Y., Zhang, X., Yin, G., Lin, W., and Yan, R. Polarquant: Leveraging polar transformation for efficient key cache quantization and decoding acceleration. *arXiv preprint arXiv:2502.00527*, 2025.

Xiao, G., Tian, Y., Chen, B., Han, S., and Lewis, M. Efficient streaming language models with attention sinks. *arXiv preprint arXiv:2309.17453*, 2023.

Xiao, G., Tang, J., Zuo, J., Guo, J., Yang, S., Tang, H., Fu, Y., and Han, S. Duoattention: Efficient long-context llm inference with retrieval and streaming heads. *arXiv preprint arXiv:2410.10819*, 2024.

Yang, A., Li, A., Yang, B., Zhang, B., Hui, B., Zheng, B., Yu, B., Gao, C., Huang, C., Lv, C., et al. Qwen3 technical report. *arXiv preprint arXiv:2505.09388*, 2025.

Zeng, A., Lv, X., Zheng, Q., Hou, Z., Chen, B., Xie, C., Wang, C., Yin, D., Zeng, H., Zhang, J., et al. Glm-4.5: Agentic, reasoning, and coding (arc) foundation models. *arXiv preprint arXiv:2508.06471*, 2025.

Zhang, H., Ji, X., Chen, Y., Fu, F., Miao, X., Nie, X., Chen, W., and Cui, B. Pqcache: Product quantization-based kvcache for long context llm inference. *Proceedings of the ACM on Management of Data*, 3(3):1–30, 2025.

Zhang, Z., Sheng, Y., Zhou, T., Chen, T., Zheng, L., Cai, R., Song, Z., Tian, Y., Ré, C., Barrett, C., et al. H2o: Heavy-hitter oracle for efficient generative inference of large language models. *Advances in Neural Information Processing Systems*, 36:34661–34710, 2023.

A. Proof of Theorem 4.1 and Gap Analysis

In this section, we provide the formal proof for Theorem 4.1 and analyze the duality gap. We first prove a sequence-length-independent upper bound, then show that the relative gap vanishes as the context length grows, and finally explain why the realized gap at the converged dual variable is typically much tighter than the worst-case bound.

A.1. Proof of Theoretical Bound

Recall the primal problem P^* in Eq. (1) and its dual D^* in Eq. (2).

Proof of Theorem 4.1. The problem consists of N separable terms subject to $m = 1$ linear constraint. The **Shapley-Folkman-Starr Theorem** (Starr, 1969) implies that the duality gap of a separable problem with m linear constraints can be bounded by the sum of non-convexities of at most m terms.

Since we have exactly one constraint ($m = 1$), the gap is bounded by the non-convexity of a single term:

$$P^* - D^* \leq \max_{i=1,\dots,N} \rho(L_i) =: \Delta. \quad (4)$$

Here, $\rho(L_i)$ denotes the maximum deviation between L_i and its convex envelope on the convexified domain $\text{conv}(\mathcal{D})$. Crucially, this bound Δ depends only on the properties of a single token’s loss function. Therefore, Δ is a **constant** that remains **independent of the sequence length** N . \square

A.2. Vanishing Relative Error

This analysis suggests that the relative impact of the duality gap diminishes as the context length increases. Since the primal objective $P^*(N)$ is the summation of losses over N tokens, the total value naturally grows with the sequence length (i.e., $P^* \approx O(N)$).

When comparing the bounded absolute gap against this growing total loss, the relative error tends to become negligible:

$$\frac{\Gamma}{P^*(N)} \approx O\left(\frac{1}{N}\right) \rightarrow 0 \quad \text{as } N \rightarrow \infty. \quad (5)$$

This indicates that for long-context scenarios, the solution provided by the Lagrangian relaxation is asymptotically near-optimal.

A.3. Gap Tightness at Converged λ^*

While the theorem guarantees that the gap does not scale with N , the theoretical constant Δ is a worst-case upper bound. Theoretically, the non-convexity ρ could be as large as the total loss of a significant token (“loss jump”), which might suggest a potentially loose bound.

However, in practice, the duality gap is determined by the specific dual variable λ^* to which our algorithm converges. Let \hat{d} be the final *feasible* allocation returned by our algorithm and let $D(\lambda)$ be the dual objective. By weak duality, for any $\lambda \geq 0$ we have $D(\lambda) \leq D^* \leq P^* \leq P(\hat{d})$, hence

$$\Gamma = P^* - D^* \leq P(\hat{d}) - D(\lambda^*) =: \bar{\Gamma}(\lambda^*). \quad (6)$$

In Section A.4, we verify that the realized bound $\bar{\Gamma}(\lambda^*)$ is typically much smaller than the worst-case Δ .

A.4. Empirical Verification

We validate this analysis on the **MultiFieldQA-en** dataset from the **LongBench** benchmark. We sample sequences of varying lengths and evaluate the duality gap using **Llama-3-8B-Instruct**.

Table 4 presents the results:

- **Primal Loss ($P(\hat{d})$):** As expected, the total objective value grows with context length (from 63.83 to 104.59).

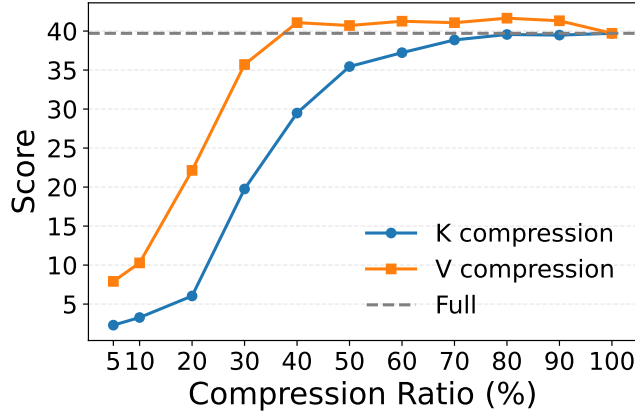


Figure 7. Performance of MultiFieldQA-en under different KV compression ratios.

- **Gap Upper Bound ($\bar{\Gamma}(\lambda^*)$):** The upper bound of duality gap $P(\hat{d}) - D(\lambda^*)$ remains small and shows no systematic growth with N .

Consequently, the relative gap drops to below 0.15% for longer sequences, supporting the effectiveness of our approach for long-context tasks.

In addition to the sequence-level averages in Table 4, Table 5 shows that this tightness holds *across layers* as well, indicating it remains small for the vast majority of layers.

Table 4. Scalability of Duality Gap (MultiFieldQA-en from LongBench).

Context Length (N)	Avg. Primal Loss ($P(\hat{d})$)	Avg. Gap Upper Bound ($\bar{\Gamma}(\lambda^*)$)	Avg. Relative Gap (%)
2,005	63.83	0.023	0.033%
4,752	71.26	0.010	0.015%
6,186	104.59	0.010	0.011%

Table 5. Layer-wise Statistics (at $N = 6, 186$).

Metric	Min	25th Percentile	Median	75th Percentile	Max
Sensitivity (λ^*)	1.3×10^{-5}	9.3×10^{-5}	1.7×10^{-4}	2.2×10^{-4}	4.2×10^{-4}
Relative Gap (%)	0.000%	0.000%	0.000%	0.010%	0.085%

B. Parameter Choice

For most experiments of our solution, we set the candidate set of compression ratios to $\{0\%, 12.5\%, 25\%, 100\%\}$. We evaluate the performance of KV dimensional reduction for Llama-3-8B-Instruct in one of the LongBench datasets (MultiFieldQA-en), where we vary the compression ratio for keys or values and report the scores. As shown in Figure 7, we observe a performance drop when the compression ratio is lower than 50%. When selecting the optional compression ratios, the 0% is selected to achieve low KV budget, and the 100% is selected to maintain the important information. Then We aim to select dimensions that yield substantial compression benefits while avoiding severe information loss caused by compressing important tokens along those dimensions. The optional dimensions should be powers of two, and the number of candidate options is kept limited to avoid computational fragmentation. We find that at 50% the performance degradation is noticeable but not severe, making the cost of compression difficult to distinguish; however, compressing important tokens to this dimensionality can still incur non-negligible information loss. Therefore, we skip 50% and choose 25% and 12.5%.

Table 6. Additional results on LongBench.

Method	Single-Doc QA			Multi-Doc QA			Summarization			Few-shot Learning			Synthetic		Code		Avg.
	NQA	Qasper	MF-en	HQA	2WQA	Musq	GRep	QMSum	MNews	TREC	TQA	SAMSum	PCount	Pre	Lcc	RB-P	
<i>Llama-3-8B-Instruct KV size = 256</i>																	
Full	25.56	32.30	39.71	43.56	35.49	21.14	28.58	23.22	26.67	74.00	90.48	42.29	4.80	69.75	59.13	54.02	41.92
H2O	23.09	18.56	29.02	36.01	28.07	15.70	23.31	21.48	24.57	60.50	88.70	38.55	5.37	68.04	58.52	52.73	37.01
SnapKV	23.36	20.2	37.36	42.37	33.18	19.96	21.76	22.00	22.83	71.00	90.86	40.03	5.83	69.50	60.16	55.91	39.77
Pyramid	23.99	20.51	36.06	42.47	31.34	20.28	21.36	22.68	22.83	71.00	90.48	39.86	5.83	69.25	58.64	54.06	39.42
MD	25.26	31.39	39.60	43.82	35.46	21.59	27.07	22.95	26.54	73.00	90.61	42.40	5.02	69.50	59.11	54.84	41.76
<i>Mistral-7B-Instruct KV size = 256</i>																	
Full	29.07	41.54	52.88	49.37	39.01	28.58	35.07	25.71	27.73	76.00	88.59	47.51	6.00	98.50	61.48	62.68	48.11
H2O	25.93	34.24	42.34	46.22	33.65	22.8	26.90	21.61	25.89	72.50	87.69	40.96	6.50	88.00	53.94	47.76	42.31
SnapKV	27.72	33.18	51.59	47.58	37.60	27.73	23.98	23.12	23.21	73.00	88.79	44.88	5.00	96.00	58.05	58.12	44.97
Pyramid	27.60	33.36	52.23	48.48	38.11	27.10	23.64	23.20	23.25	72.50	89.56	45.14	5.50	96.00	56.90	55.62	44.89
MD	29.62	41.50	53.05	48.49	38.70	28.16	30.67	25.33	27.59	75.00	88.75	47.81	6.00	98.00	61.44	62.30	47.65

C. Extended Experimental Results

In this section, we provide additional experimental results to complement the analysis in the main text. In Section C.1 and Section C.2, we present additional results on LongBench and RULER, respectively. In Section C.4 we show the results of Needle-in-a-Haystack tests on the Mistral model.

C.1. More Results on LongBench

In Table 6 we supplement the experimental results with a KV size of 256 on the LongBench. The results show that our solution achieves a consistent performance improvement compared with H2O, SnapKV, and PyramidKV. In Table 7 we present the full results of HeadKV and MixedDimKV-H on LongBench.

C.2. More Results on RULER

In Table 8 we present the full results on RULER.

C.3. Comparison with Dimension Reduction Methods

We benchmark our approach against dimension reduction-based methods to provide a comprehensive evaluation. We select Palu (Chang et al., 2024) as the representative baseline for this category due to its clear implementation and reproducibility. Unlike eviction strategies that discard tokens, Palu performs low-rank decomposition on the linear projection matrices (W_k, W_v), effectively reducing the hidden dimension of the KV cache while retaining all tokens.

Setup. To ensure a fair comparison, we align the total memory footprint of the KV cache for both methods. Specifically, we set the token budget of our MixedDimKV and MixedDimKV-H variants to 10% of the prefill sequence length. Correspondingly, we adjust the projection dimension in Palu to a specific ratio that yields an identical KV cache size (i.e., a 40% projection dimension).

Results. As shown in Table 9, Palu experiences a significant performance degradation at this compression level. In contrast, our solution demonstrates superior resilience, maintaining performance comparable to the full-cache baseline.

C.4. Needle-in-a-Haystack tests on Mistral

We evaluate the Needle-in-a-Haystack test on the Mistral-7B-Instruct-v0.2 model. We set the maximum context length to 32K, the KV size to 128, and the query window size to 16. As shown in Figure 8, MixedDimKV significantly outperforms the baselines that does not relies on additional head-level information (SnapKV, PyramidKV). Equipped with the same

Beyond Token Eviction: Mixed-Dimension Budget Allocation for Efficient KV Cache Compression

Table 7. Full LongBench results for HeadKV and MixedDimKV-H (MD-H).

Method	Single-Doc QA			Multi-Doc QA			Summarization			Few-shot Learning			Synthetic		Code		Avg.
	NQA	Qasper	MF-en	HQA	2WQA	Musq	GREp	QMSum	MNews	TREC	TQA	SAMSum	PCount	Pre	Lcc	RB-P	
<i>Llama-3-8B-Instruct KV size = 128</i>																	
Full	25.56	32.30	39.71	43.56	35.49	21.14	28.58	23.22	26.67	74.00	90.48	42.29	4.80	69.75	59.13	54.02	41.92
HeadKV	22.56	28.04	39.64	44.40	31.83	20.62	22.16	23.04	24.04	71.00	90.10	38.81	4.89	68.75	61.72	61.77	40.84
MD-H	24.59	27.15	41.39	43.59	35.10	20.59	23.43	22.74	25.56	70.00	90.34	40.51	5.08	69.50	62.30	59.69	41.35
<i>Llama-3-8B-Instruct KV size = 256</i>																	
Full	25.56	32.30	39.71	43.56	35.49	21.14	28.58	23.22	26.67	74.00	90.48	42.29	4.80	69.75	59.13	54.02	41.92
HeadKV	24.53	30.52	38.46	43.99	35.62	20.60	23.33	22.85	24.97	72.50	90.43	40.13	6.03	69.75	62.12	61.14	41.69
MD-H	24.85	30.13	40.45	44.22	36.24	20.74	26.04	23.01	26.05	73.00	90.56	41.32	5.64	69.50	62.44	59.84	42.13
<i>Llama-3-8B-Instruct KV size = 512</i>																	
Full	25.56	32.30	39.71	43.56	35.49	21.14	28.58	23.22	26.67	74.00	90.48	42.29	4.80	69.75	59.13	54.02	41.92
HeadKV	24.83	29.85	38.06	44.30	36.34	22.17	24.70	23.14	26.03	73.50	90.56	40.82	5.66	69.50	62.36	60.66	42.03
MD-H	25.37	31.96	39.82	43.97	36.91	21.39	27.61	23.35	26.24	73.50	90.64	41.83	5.27	69.50	62.02	58.29	42.35
<i>Mistral-7B-Instruct KV size = 128</i>																	
Full	29.07	41.54	52.88	49.37	39.01	28.58	35.07	25.71	27.73	76.00	88.59	47.51	6.00	98.50	61.48	62.68	48.11
HeadKV	27.23	37.88	52.46	47.74	38.95	27.69	26.15	24.12	24.32	75.00	90.11	44.35	4.50	94.5	58.93	57.95	45.74
MD-H	28.22	38.08	51.12	48.79	37.75	27.32	27.38	24.73	26.63	66.50	90.11	44.95	5.23	98.00	61.14	60.38	46.02
<i>Mistral-7B-Instruct KV size = 256</i>																	
Full	29.07	41.54	52.88	49.37	39.01	28.58	35.07	25.71	27.73	76.00	88.59	47.51	6.00	98.50	61.48	62.68	48.11
HeadKV	28.62	39.27	52.56	50.78	38.80	28.56	28.49	24.38	26.23	75.50	89.52	44.93	5.50	97.00	60.41	61.43	47.00
MD-H	29.34	39.96	53.14	49.60	38.78	28.32	30.84	24.73	27.30	75.00	89.86	46.41	5.50	97.50	61.66	62.65	47.54
<i>Mistral-7B-Instruct KV size = 512</i>																	
Full	29.07	41.54	52.88	49.37	39.01	28.58	35.07	25.71	27.73	76.00	88.59	47.51	6.00	98.50	61.48	62.68	48.11
HeadKV	27.23	37.88	52.46	47.74	38.95	27.69	26.15	24.12	24.32	75.00	90.11	44.35	4.50	94.5	58.93	57.95	45.74
MD-H	28.22	38.08	51.12	48.79	37.75	27.32	27.38	24.73	26.63	66.50	90.11	44.95	5.23	98.00	61.14	60.38	46.02

head-level information, MixedDimKV-H also outperforms HeadKV. We further find that in Mistral MixedDimKV achieves a better score compared with HeadKV and MixedDimKV-H, which indicates that HeadKV still has limitations in evaluating the importance of attention heads.

C.5. More Results on Dimension Allocation

For most experiments, the candidate set of dimension compression ratios is set to $\{0\%, 12.5\%, 25\%, 100\%\}$. We report the average token length and the proportion of tokens allocated to each compression ratio, averaged over all layers and samples in each dataset. Figure 9 presents the results on different LongBench datasets. We find that all four compression ratios take effect by allocating a portion of tokens. Specifically, tokens are predominantly allocated to the 0% and 100% compression ratios, while the two intermediate ratios account for a non-negligible 10%-15% of the total tokens, which improves the space utilization of the KV cache. Notably, in longer datasets, an even larger proportion of tokens are assigned to the 0% ratio, which is a direct consequence of the constrained budget setting.

Table 8. Full results of our solution and baselines on RULER.

Method	S1	S2	MK1	MK2	MQ	MV	VT	QA-1	QA-2	Avg.
<i>Context Length = 8K</i>										
Full	100	100	99.4	99.4	99.25	83.4	96.64	69.83	58.4	89.59
H2O	1.8	0.2	0.4	3	0.05	0.3	15.76	36.8	32.8	10.12
SnapKV	100	98.2	96.8	92	75.95	71.9	80.52	63.93	50	81.03
PyramidKV	100	98	96.8	93	74.6	72.05	84.16	60.28	50	80.99
HeadKV	100	99.2	99.2	99	98.85	94.75	89.92	65.6	55.2	89.08
MixedDimKV	99.6	99.4	98.8	95.6	88.4	80.25	97.52	67.62	57.4	87.18
MixedDimKV-H	100	99.6	98.4	97.4	96.5	89.7	97.28	68.78	57.6	89.47
<i>Context Length = 32K</i>										
Full	99.60	98	98	97	46.6	94.15	22.28	69.78	53.2	75.40
H2O	0.8	0	0	0	0	0	4.04	24.2	23.6	5.85
SnapKV	100	85.8	89.8	13.6	7.25	16.5	20.88	62.77	45.8	49.16
PyramidKV	100	80.6	78.8	14.4	3.69	5.05	20.48	60.27	44.6	45.31
HeadKV	100	90.6	92	44	24.8	56.5	20.92	64.27	50.8	60.43
MixedDimKV	98.40	85.60	92.4	8.4	7.75	17.1	21.24	66.47	51.2	49.84
MixedDimKV-H	100	95.2	96	38.4	31.05	64.35	21.6	65.80	51.4	62.64

Table 9. Comparative analysis with PALU on LongBench.

Method	Single-Doc QA			Multi-Doc QA			Summarization		Few-shot Learning			Synthetic		Code		Avg.	
	NQA	Qasper	MF-en	HQA	2-WQA	Musq	GRep	QMSum	MNews	TREC	TQA	SAMSum	PCount	PRE	Lcc		RB-P
<i>Llama-3-8B-Instruct Budget = 10%</i>																	
Full	25.56	32.30	39.71	43.56	35.49	21.14	28.58	23.22	26.67	74.00	90.48	42.29	4.80	69.75	59.13	54.02	41.92
Palu	15.44	9.32	19.22	17.82	16.87	8.65	9.74	20.21	14.08	45.00	22.89	23.32	1.59	4.35	7.82	9.07	15.34
MD	25.22	28.55	38.67	43.39	32.42	21.13	25.72	23.12	25.96	72.00	90.48	42.74	4.90	69.25	59.16	54.23	41.06
MD-H	25.32	32.07	39.96	43.91	36.38	21.48	27.39	23.25	25.95	73.50	90.56	41.84	4.81	69.50	61.86	57.19	42.19
<i>Mistral-7B-Instruct Budget = 10%</i>																	
Full	29.07	41.54	52.88	49.37	39.01	28.58	35.07	25.71	27.73	76.00	88.59	47.51	6.00	98.50	61.48	62.68	48.11
Palu	22.12	31.68	42.54	37.03	28.45	20.08	18.66	22.90	23.98	70.00	80.96	35.66	4.50	22.00	33.72	33.28	32.97
MD	29.12	38.12	52.89	49.01	39.48	28.24	30.81	25.60	25.89	74.00	88.59	47.30	6.00	98.50	61.75	62.54	47.37
MD-H	29.16	41.00	53.84	49.58	38.96	28.48	34.10	25.78	27.03	76.00	88.59	47.18	6.00	98.50	61.56	62.54	48.02

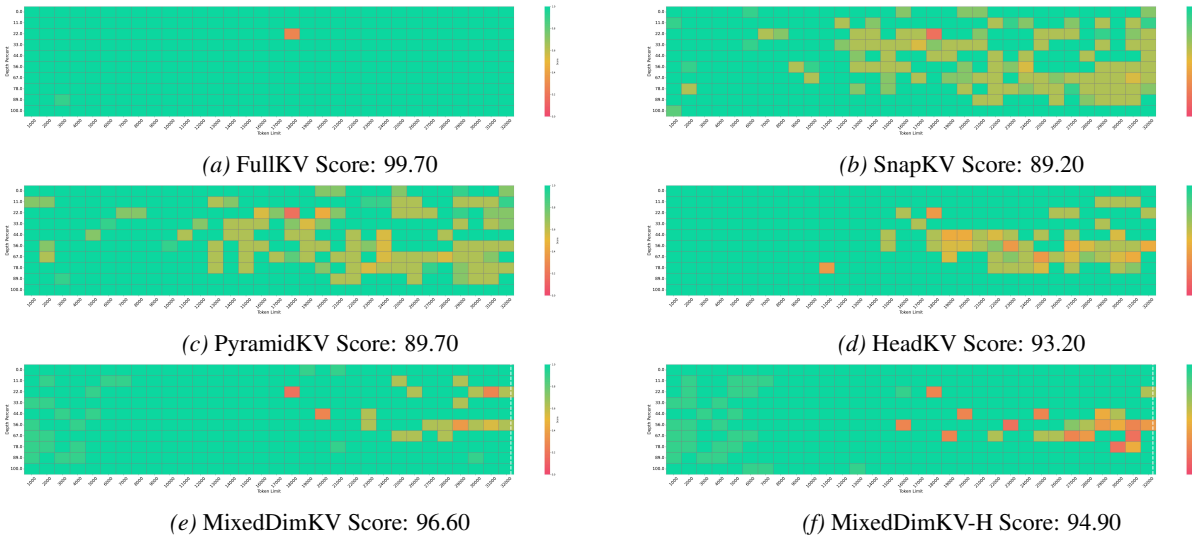


Figure 8. Results of Needle-in-a-Haystack test on Mistral-7B-Instruct with KV size 128.

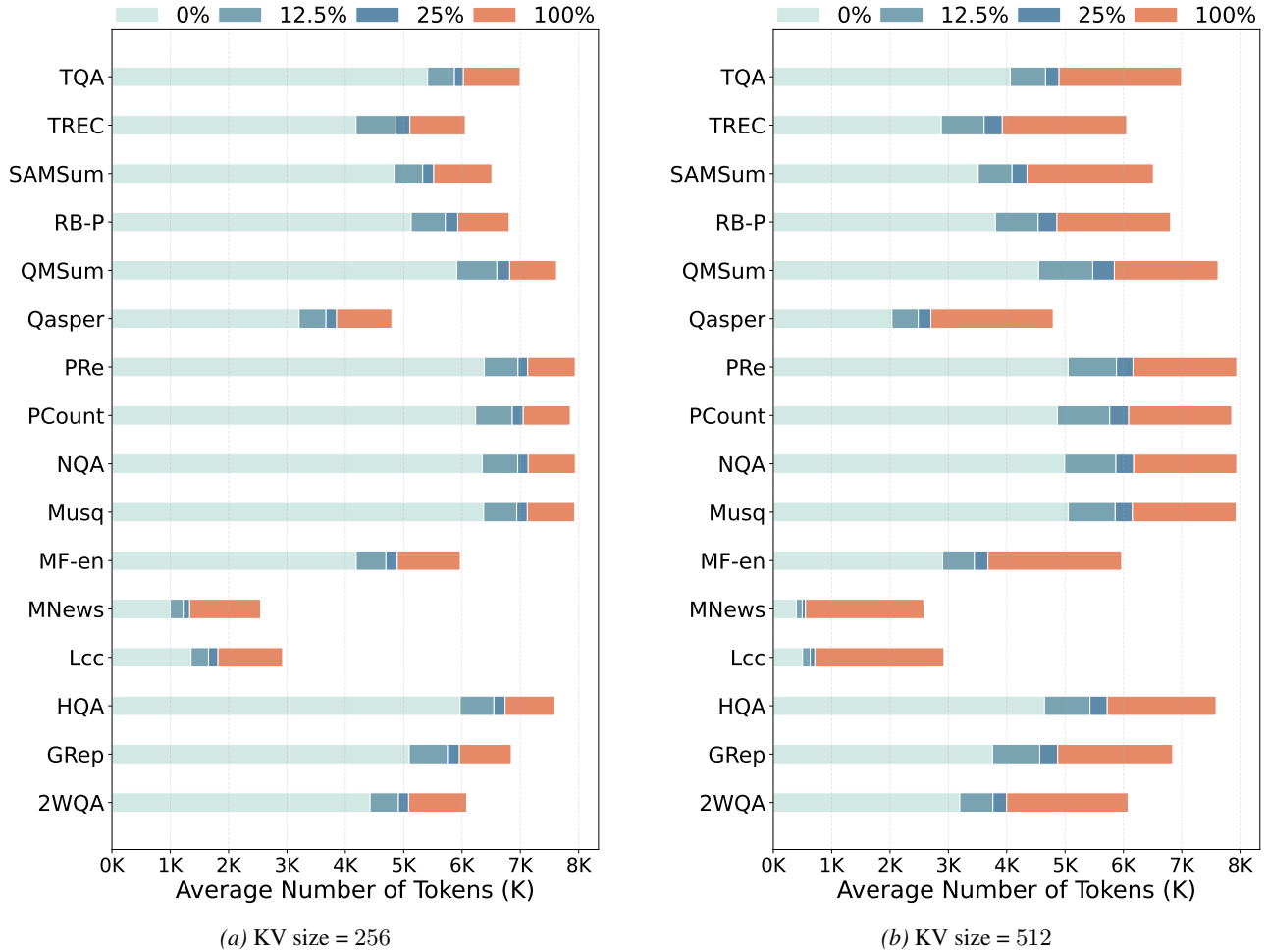


Figure 9. Average number of tokens and the allocation statistics across candidate compression ratios on LongBench.